DIGITAL ACCESS TO SCHOLARSHIP AT HARVARD
DASH.HARVARD.EDU

HARVARD LIBRARY

ALD Growth of MgxCa1xO on GaN and Its Band Offset Analysis

Citation

Gong, Xian, Lou, Xiabing, Kim, Sang Bok, and Gordon, Roy G. "ALD Growth of Mg X Ca1–x O on GaN and Its Band Offset Analysis." ACS Applied Electronic Materials 3, no. 2 (2021): 845-53.

Published version

https://doi.org/10.1021/acsaelm.0c00977.s001

Link

https://nrs.harvard.edu/URN-3:HUL.INSTREPOS:37367260

Terms of use

This article was downloaded from Harvard University's DASH repository, and is made available under the terms and conditions applicable to Open Access Policy Articles (OAP), as set forth at
https://harvardwiki.atlassian.net/wiki/external/NGY5NDE4ZjgzNTc5NDQzMGIzZWZhMGFlOWI2M2EwYTg

Accessibility

https://accessibility.huit.harvard.edu/digital-accessibility-policy

Share Your Story

The Harvard community has made this article openly available.
Please share how this access benefits you. Submit a story

ALD growth of $Mg_xCa_{1-x}O$ on GaN and its band offset analysis

*Xian Gong‡, Xiabing Lou‡, Sang Bok Kim, Roy G. Gordon**

X. Gong, Prof. Roy G. Gordon
John A. Paulson School of Engineering and Applied Sciences
Harvard University
Cambridge, Massachusetts 02138, United States

X. B. Lou, S.B. Kim, Prof. Roy G. Gordon
Department of Chemistry and Chemical Biology
Harvard University
Cambridge, MA 02138, USA

Keywords: GaN, $Mg_xCa_{1-x}O$, band offset, ALD, crystallinity

Abstract:

Atomic layer deposition (ALD) processes were developed for growing MgO and CaO on GaN substrates using a home-built ALD reactor with amidinate based precursors. An optimal deposition condition was then determined to deposit pure $Mg_xCa_{1-x}O$ by tuning deposition temperature, achieving a high quality film without carbon and hydroxyl contamination. Band offset analysis was conducted by X-ray Photoelectron spectroscopy (XPS) on $Mg_xCa_{1-x}O$/GaN samples with various compositions. $Mg_{0.25}Ca_{0.75}O$/GaN demonstrated band alignments between defect free and fully pinned while other ratios showed near fully pinned alignments, which agrees with the best electrical properties achieved in our previous studies. This result indicates band offset analysis provides a good aid in understanding part of the electrical and interfacial properties for oxide/semiconductor structures.

Introduction:

GaN has been regarded as the next generation semiconductor for high power, high frequency applications at elevated temperature. However, traditional dielectrics such as SiO_2, HfO_2, and native oxide Ga_2O_3 cannot achieve a high-quality interface on a GaN substrate, unlike a silicon substrate.[1] Previously, a mixture of MgO and CaO has been proposed to achieve a lattice matched, low defect epitaxial dielectric film. Although MgO and CaO are immiscible thermodynamically below 2000°C, a kinetically stable $Mg_xCa_{1-x}O$ film has been achieved with e-beam evaporation(EE)[2-4]and molecular beam epitaxy (MBE). [5] However, the surface of an EE deposited $Mg_xCa_{1-x}O$ film is rough which cannot be used for dielectric applications while the MBE method is not compatible with industrial production due to its ultra-high vacuum requirement. Atomic Layer Deposition (ALD) method is advantageous in achieving well controlled smooth films and its low vacuum requirement guarantees its mass production feasibility. Moreover, the typical lower deposition temperature of ALD process can prevent the alloy film from phase separation. ALD processes for MgO and CaO have already been developed separately[6-7], however, the deposition temperatures are usually very high due to the high reaction temperature of the precursors. In addition, since $Mg_xCa_{1-x}O$ is thermodynamically unstable, a lower deposition temperature (<400°C) is desirable for high quality, uniform films. Therefore, new ALD precursors and processes should be developed for MgO and CaO with lower deposition temperatures under 400 °C.

ALD MgO has been achieved with a variety of precursors for different applications.[6] $Mg(C_2H_5)_2$ and H_2O were first employed for ALD MgO at above 600°C.[8] The commercially available $Mg(Cp)_2$ and similar precursors can react with H_2O at lower temperatures but the films are usually amorphous below 400°C.[9-12] Thus, these Mg precursors are not suitable for our ALD $Mg_xCa_{1-x}O$ process.

Previously, pure CaO film has been achieved by post annealing ALD $CaCO_3$ film from calcium β-diketonate, CO_2 and ozone precursors.[13] CaO obtained through this process is not capable of achieving an alloy with MgO. CaO film from direct ALD reaction has been reported using Ca(1,2,4-tri-isopropylcyclopentadienyl)$_2$ and H_2O as precursors.[7] However, due to the relatively low reactivity of the Ca precursor and the high water reactivity of CaO, the resulting film contains a considerable concentration of hydroxyl groups and carbon contamination. Therefore, this process is not ideal for deposition of high quality epitaxial $Mg_xCa_{1-x}O$. To deposit highly crystalline and pure CaO by ALD, a Ca precursor with high-water reactivity and low carbon contamination is needed.

Amidinate based precursors are known for high thermal stability and high reactivity with water. The high thermal stability can reduce carbon contamination from side reactions and the high reactivity can reduce the residual hydroxyl groups and further improve the crystallinity at lower deposition temperature.[14] The higher reactivity between water and amidinate ligand-based precursors is mainly due to the highly strained, four membered ring structure. Compared to the oxygen-metal bond, the weaker nitrogen-metal bond also makes the ligand easier to leave and therefore results in less carbon contamination. Acetamidinate Ca precursor has been reported to be stable at high temperature (above 300C), and relatively high volatility. Thus, we choose to use amidinate ligand-based Mg and Ca precursors in this study.

Previously, we demonstrated that ALD MgCaO/GaN can achieve a low interfacial trap density and a high performance HEMT device based on this structure.[15] In this work, the ALD depositions

of MgO and CaO with amidinate precursors are carefully studied. An optimal condition for ALD $Mg_xCa_{1-x}O$ is determined by tuning the deposition temperature to prevent hydroxyl and carbon residues from formation. Lower deposition temperatures near 300℃ are successfully achieved and high quality, stable and crystalline ALD $Mg_xCa_{1-x}O$ films are developed. Moreover, X-ray photoelectron spectroscopy (XPS) has been employed to study the relationship between MgCaO composition and band offset.

Experiment section

GaN substrate and surface pretreatment

Epi-layers GaN (3 inches diameter, 5 μm thick) grown on sapphire are used as substrates, which were purchased from MTI with resistivity of 0.02 Ω·cm. Prior to deposition, a 5 min UV-Ozone treatment is performed to remove the adsorbed organic contaminations. Then the substrate is immersed with Buffered Oxide Etchant (BOE 1:6) for 30s followed by 20min soaking in 20% ammonium hydroxide solution to remove native oxide.

Film deposition

In this study, bis(N,N'-di-sec-butylacetamidinato) magnesium (Figure S1) and bis(N,N'-diisopropylacetamidinato)calcium(II) dimer (Figure S2) were used for MgO and CaO deposition, respectively. Water vapor H_2O was used as the oxygen source. The ALD process was carried out in our home-built reactor (Figure S3). The Mg precursor was kept in a sealed bubbler at 110°C while the Ca precursor was placed in a glass bubbler kept in a heated oven at 140°C. The metal precursors were then delivered into the reaction chamber with controlled volumes of N_2 carrier gas. The substrate deposition temperature varied from 220 °C to 340 °C. The pressure during the ALD process was maintained at 0.3 Torr. ALD of $Mg_xCa_{1-x}O$ thin films was conducted using a

supercycle composed of combinations of subcycles of MgO and CaO ALD. The cation composition of $Mg_xCa_{1-x}O$ thin films was controlled by changing the subcycle ratio between MgO and CaO.

Characterization

The film thickness was characterized by X-ray reflectivity (XRR) with the Bruker Discover D8 system. Chemical status and the band alignment of our films were investigated by Thermo Scientific K-Alfa X-ray photoelectron spectroscopy (XPS). A JEOL 2100 transmission electron microscope (TEM) was used to study microscopic crystallography and epitaxy relation of our films. Our films were deposited onto a TEM grid with an ultrathin silicon nitride membrane for the crystallinity study. Cross-sectional samples were prepared with a FEI Helios 660 focused ion beam (FIB) system for epitaxy investigation. Fourier-transform infrared spectroscopy (FTIR) spectrum of our films was carried out with a Bruker FT-IR Microscope to check for hydroxyl groups.

Result and discussion

3.1 MgO deposition study

The growth rates of MgO at different substrate temperatures are summarized in Figure 1(a). The growth rate is obtained by the X-ray reflectivity (XRR) measured thickness divided by the total ALD cycles. (Figure S4) A growth rate between 0.67~0.5 Å per cycle has been achieved ranging from 140°C to 320°C. The growth rate slightly decreases with an increasing substrate temperature. The large ALD window confirmed the high reactivity and thermal stability of this precursor.

$Mg(OH)_2$ is thermodynamically stable at room temperature. The Gibbs free energy of $MgO + H_2O \rightarrow Mg(OH)_2$ is -48.4 kJ/mol at room temperature. $Mg(OH)_2$ will thermally decompose into MgO and H_2O vapor at above 330ºC. This temperature should be even lower under vacuum condition. Therefore, the reactivity of the Mg precursor needs to be high enough to deplete the hydroxyl groups after each H_2O dose to prevent $Mg(OH)_2$ formation at low deposition temperature. Figure 1(b) summarized the Fourier-transform infrared spectroscopy (FTIR) spectrum of MgO deposited at different temperatures. The absence of OH stretching at around 3700 cm^{-1} indicates that there is no detectable hydroxyl group in a wide temperature range.

Figure 2 summarizes the X-ray photoelectron spectrum fine scan of Mg 2s and O 1s binding energy peaks. Since MgO is an insulating material, binding energies may shift as large as 1eV during the sputtering process. The positions of Mg 2p peaks in different samples are ranging from 49.6 eV to 50.3 eV. The well-defined Gaussian peaks of Mg 2p indicate that there is no metallic Mg in the film. This is consistent with pure MgO XPS.[12] The O 1s peaks are ranging from 530.5 eV to 530.9 eV and in good consistency with MgO. The absence of OH peak at around 533 eV confirmed that all the films are hydroxyl group free. On the other hand, the carbon peaks are almost undetectable in XPS, which indicate that the carbon contamination is below 1%.

To confirm the crystallinity of ALD MgO, a thin film was deposited on Si_3N_4 membrane at 190ºC and examined in TEM. In Figure 3, the high resolution TEM image shows the well crystallized grains. The grain sizes are around 10 nm which is similar to the film thickness. The well-defined rings in the diffraction pattern of Figure 3 (b) also confirmed the high crystallinity of the MgO film at such a low deposition temperature. A cross sectional TEM study of MgO/GaN(0001) shows

that polycrystalline MgO is achieved on GaN substrate. In Figure 3 (c), two layers of MgO film are visible. One possible explanation is that there is a large tensile stress between MgO and GaN near the interface resulting in the strain of MgO lattice. This is confirmed by the diffraction pattern in Figure 3 (d) in which the splitting of MgO spots clearly indicate that there are two sets of crystalline patterns with different lattice parameters. The closer-to-interface MgO layer is stressed while the top layer is relaxed. Moreover, although the film is mostly polycrystalline, some degree of epitaxy relation has been achieved as (111) × [0−11] MgO //GaN(0001) × [11−20].

3.2 CaO deposition study

The temperature dependence of the growth rate was conducted as shown in Figure 4(a). The growth rate increases from 0.4 Å/cyc to 0.75 Å/cyc with an increasing substrate temperature from 220°C to 310°C. Then the growth rate decreases to 0.6 Å at 325°C and 340°C. The decrease of growth rate above 310°C indicates a potential thermal decomposition on the substrate.

FTIR is employed to check whether $Ca(OH)_2$ is formed in the ALD CaO film. Figure 4(b) summarizes the IR reflectance spectrum ranging from 3200 cm^{-1} to 4000 cm^{-1} of CaO films deposited at different temperatures. The CaO films are 20 nm thick with a 5 nm amorphous ALD Al_2O_3 protection layer. The expected OH group stretching absorption was only showed in the sample prepared at 230°C. This indicates that the acetamidinate Ca precursor is not reactive enough to deplete the excessive hydroxyl groups below 230°C. The adsorption position accords with the OH peak in pure $Ca(OH)_2$ film.[16]

Although the IR spectrum is sensitive to hydroxyl groups, the small thickness of the thin CaO films may decrease the sensitivity of this method. Moreover, IR spectrum is not suitable for quantifying the composition of CaO film in this case. Therefore, XPS is employed to further study the temperature dependence of the film composition. Figure 5(a) shows the carbon content of CaO films deposited at different temperatures measured by XPS. Carbon contamination starts to increase at above 310°C indicating that the precursor starts to decompose beyond this temperature. At 340°C, the carbon contamination increases to 3 at%. Therefore, the deposition temperature should not exceed 310°C. Figure 5(b) demonstrates O1s scan of three CaO samples deposited at different temperatures. The main peak around 529.1 eV is from pure CaO.[17] Since Al_2O_3 is employed as a protection layer, an O1s peak of Al_2O_3 showed up at 530.3eV potentially due to either preferential etching or re-deposition during the sputtering.[18] The peak of hydroxyl group should be about 3eV shifted to a higher binding energy, in this case it is 532.1eV(labeled with blue dashed line). According to the deconvolution result, about 17% and 10% oxygen atoms are from OH groups in samples deposited at 253°C and 290°C, respectively. This peak is not visible at 310°C deposition temperature. Thus, a deposition temperature above 310°C is necessary to completely remove the OH residues.

TEM is employed to check the crystallinity of the CaO films. Similar to the TEM for MgO film, a thin layer of CaO film was deposited on Si_3N_4 membrane covered with protective Al_2O_3 film. Two samples deposited at 310°C and 273°C are prepared. As shown in Figure 6(b), the film deposited at 273°C does not show clear features of crystal grains in the HR image and the diffraction pattern is blurred. Because the $Ca(OH)_2$ crystal structure is hexagonal, it may prevent the crystallization of rocksalt CaO. On the other hand, the film deposited at 310°C shows very well crystallized grains

in the HR image and well-defined rings in diffraction. This result indicates that eliminating OH residue is critical to achieve well crystallized CaO films. The formation Gibbs energy of $Ca(OH)_2$ from CaO and H_2O at room temperature is -66.3kJ/mol and the decomposition temperature is as high as 512°C at the atmospheric pressure.[19] Therefore, the absence of OH group at a higher temperature is mainly due to the completion of the ALD reaction instead of thermal decomposition of $Ca(OH)_2$. Cross sectional TEM shows the CaO film deposited on GaN under 313°C is highly textured with some extend of lattice strain. In Figure 6 (e), the diffraction spot from CaO (111) and (200) are in line shape instead of distinct spot, indicating there is a gradient of strain from bottom to top. This is different with the case of MgO/GaN in which the strained and relaxed layers are distinctive. Furthermore, although the film is mostly textured, some degree of epitaxy relation has been achieved as (111) × [0−11] CaO //GaN(0001) × [11−20].

3.3 $Mg_xCa_{1-x}O$ deposition study

$Mg_xCa_{1-x}O$ thin film has been used as a cathode luminescence material in the plasma display panel industry.[2, 20] The growth method, optical and structural properties of this material have been discussed in several publications. [4, 21]Previously, the studies were focused on the EE and MBE prepared $Mg_xCa_{1-x}O$ films. As discussed before, these deposition methods are either incapable of high-quality film growth or incompatible with mass production, thus they cannot fulfill requirement of high-k deposition for high power electronics. In previous sections we have already demonstrated that high quality MgO and CaO can be achieved by scalable ALD processes. Furthermore, MgO and CaO deposition conditions have been studied and the optimal conditions for achieving low contamination, high crystallinity film has been determined for each precursor.

To guarantee these qualities for CaO and MgO alloy films, a 310 ºC substrate temperature is chosen based on previous separate studies. This section will be dedicated to the ALD growth study and properties of $Mg_xCa_{1-x}O$ films.

$Mg_xCa_{1-x}O$ is grown by alternating the ALD CaO cycles and MgO cycles at different dosing ratios. Table 1 summarizes the average growth rates and compositions at three different dosing ratios as well as pure MgO and CaO. The average growth rate of $Mg_xCa_{1-x}O$ does not follow a linear combination of MgO and CaO growth rates. On the other hand, the Mg elemental composition in 1:2 and 1:1 dosing ratio samples is higher than the dosing ratio, indicating that there is synergy between the CaO and MgO cycles. One explanation is that during the CaO cycle, many more OH groups are formed since CaO is more hygroscopic. In pure CaO deposition, such excessive OH groups can be depleted by the next cycle of the Ca precursor dose. In the $Mg_xCa_{1-x}O$, if the next step is the Mg precursor dose, such excessive OH groups will react with the Mg precursors and therefore result in higher Mg content in the film.

$Mg_xCa_{1-x}O$ alloy is thermodynamically unstable below its melting point (2370ºC).[22] This is because of the large difference in ionic radius between Mg and Ca species.[23] However, $Mg_xCa_{1-x}O$ film has been reported to be kinetically stable until 600ºC.[24] In EE deposited $Mg_xCa_{1-x}O$ films, phase separated MgO and CaO species could be found. Therefore, it is very important to confirm the uniformity of ALD deposited $Mg_xCa_{1-x}O$ film. In this study, TEM is employed to check the film uniformity. **Figure 7** demonstrates the HR-TEM image and diffraction patterns of three $Mg_xCa_{1-x}O$ films with different compositions deposited on Si_3N_4 grid. The HR image with visible lattice and grains shows that the film is well crystallized. The diffraction patterns exhibit rocksalt patterns. The absence of MgO and CaO diffraction patterns confirmed the homogeneity of this film, and therefore, that our ALD process can achieve a metastable $Mg_xCa_{1-x}O$ alloy film.

3.4 Band offset study of ALD $Mg_xCa_{1-x}O$ on GaN

The quality of the dielectric/semiconductor interface plays an important role in device performance due to the fixed oxide charge, border and interface traps. Band offset is mainly determined by the density of interfacial defects which provides us a great method to investigate dielectric/ semiconductor interfacial quality. [25] Band offset of MgO on GaN was measure by several groups with XPS study.[26-27] In this work, we will apply Robertson's metal induced gap states (MIGS) theory[28] to establish the quantitative relationship between the defect levels and the band alignment on different ratio of $Mg_xCa_{1-x}O$ on GaN.

Based on the theory, the valence band offset ($\boldsymbol{\Delta E_V}$) can be extracted with the following equation:

$$\boldsymbol{\Delta E_V = \left(E_{core}^{oxide} - E_{VBM}^{oxide}\right)^{bulk\ oxide} - \left(E_{core}^{sub} - E_{VBM}^{sub}\right)^{bulk\ sub} - \left(E_{core}^{oxide} - E_{core}^{sub}\right)^{interface}} \quad (1)$$

where $\boldsymbol{\left(E_{core}^{oxide} - E_{VBM}^{oxide}\right)^{bulk\ oxide}}$ and $\boldsymbol{\left(E_{core}^{sub} - E_{VBM}^{sub}\right)^{bulk\ sub}}$ are the binding energy differences between the core levels and their respective valence band maximum for bulk oxides and bulk semiconductor substrates respectively. In the meantime, $\boldsymbol{\left(E_{core}^{oxide} - E_{core}^{sub}\right)^{interface}}$ corresponds to the binding energy difference of core levels for the interfacial samples.

With the knowledge of the band gap difference of two materials ($\boldsymbol{\Delta E_g}$) and valence band offset ($\boldsymbol{\Delta E_V}$), the conduction band offset ($\boldsymbol{\Delta E_C}$) value can be then derived from the formula (2).

$$\boldsymbol{\Delta E_C = \Delta E_g - \Delta E_V} \quad (2)$$

A detailed explanation for the above band offset theory can be referred to our previously published paper.[29] In our work, the energy differences between the core level and valence band maximum of the oxide insulator (40 nm $Mg_xCa_{1-x}O$ films) and semiconductor (cleaned GaN substrate wafer)

are measured as $\left(E_{core}^{oxide} - E_{VBM}^{oxide}\right)^{bulk\ oxide}$ and $\left(E_{core}^{sub} - E_{VBM}^{sub}\right)^{bulk\ sub}$, respectively. Then the core levels of the thin (2 nm) $Mg_xCa_{1-x}O$ film grown on GaN substrate are measured, corresponding to $\left(E_{core}^{oxide} - E_{core}^{sub}\right)^{interface}$.

Therefore, in order to determine the valence band offset (ΔE_V) and study the trend for $Mg_xCa_{1-x}O$ /GaN systems, we collected XPS spectra on samples with 5 different ratios: MgO, $Mg_{0.72}Ca_{0.28}O$, $Mg_{0.51}Ca_{0.49}O$, $Mg_{0.25}Ca_{0.75}O$, CaO. For each ratio, three various samples were measured: (1) 40 nm $Mg_xCa_{1-x}O$ /GaN, (2) 2 nm $Mg_xCa_{1-x}O$ /GaN, (3) bare GaN. Finally, ΔE_V for different ratio $Mg_xCa_{1-x}O$ /GaN can be extracted by equation (1) as described. Additionally, MgO and CaO are known to be hygroscopic in air. To protect our samples from hydroxylation during transfer between ALD reactor to XPS chamber, we deposited a 5 nm Al_2O_3 barrier layer on top of our samples. O 1s binding energy measured by the XPS was used to distinguish the metal-oxide bonds with the hydroxyl groups. Although our samples were coated with Al_2O_3 barrier layer, little composition of our oxide films were converted to hydroxyls. (shown in **Figure S5**) Few compositional impurities might affect the absolute value of band offsets, however, the relative relation and trend won't be influenced. Table 2 summarizes the binding energy differences between VBMs, core levels and the valence band offsets (ΔE_V) for each ratio. Pure MgO and CaO both showed larger ΔE_V while $Mg_{0.25}Ca_{0.75}O$ showed smallest ΔE_V.

In theory, the band offset between semiconductor and oxide can be predicted by the electron affinities (Ea) and charge neutrality levels (CNL). **Table 3** demonstrates the band properties for GaN and $Mg_xCa_{1-x}O$. The Ea and CNL are from literatures and estimated based on Vegard's Law.[30] According to the CNL model[31], the defect free and fully pinned MgO/GaN interface should have

a valence band offset of 1.11 eV and 1.68 eV respectively (shown in **Figure S8**). The two extreme cases for all other ratio $Mg_xCa_{1-x}O$ /GaN can be predicted similarly. In this paper, the defect free case refers to bands aligned with intrinsic MIGS states and the fully pinned case refers to bands pinned by extrinsic defect states.

Figure 8 shows the comparison of our XPS-measured band offsets with predicted extreme cases for five different ratio $Mg_xCa_{1-x}O$ /GaN. Band offset of $Mg_{0.25}Ca_{0.75}O$ /GaN demonstrated band alignments between defect free and fully pined case while all other ratios showed near fully pinned case. Although the band alignments measurements by XPS might not be very accurate due to its precision limit, this clear trend indicates that a better interfacial property could be achieved near $Mg_{0.25}Ca_{0.75}O$ ratio, which was confirmed by the optimal electrical and epitaxial property achieved in our previous study.[15] It is common for GaN interfaces to have defect states or a pinned Fermi level at characteristic energies because dangling bonds may lead to the surface reconstruction.[32] Other methods may measure the GaN interfacial states more precisely.[33]

Summary

In this paper, an ALD $Mg_xCa_{1-x}O$ deposition process and dosing recipe has been developed. The optimal deposition condition was determined by studying the ALD growth behavior of MgO and CaO with amidinate based precursors. XPS and IR showed that OH residue and C residue may appear at too low and too high deposition temperature, respectively. Therefore, a 310ºC substrate deposition temperature was carefully selected. Furthermore, TEM and electron diffraction were employed to investigate the crystallinity of $Mg_xCa_{1-x}O$ films with three dosing ratios. The resulting $Mg_xCa_{1-x}O$ films with all ratios showed high conformity, homogeneity and crystallinity. Band

offset analysis was carried out with all different ratio of $Mg_xCa_{1-x}O$ grown on GaN. Band alignment of $Mg_{0.25}Ca_{0.75}O$ /GaN showed band alignments between defect free and fully pinned cases while that of all other ratios demonstrated a near fully pinned case. This matched the optimal electrical measurement and interfacial properties in our previously reported study. Thus, these band offset analyses provide a good way to help understand the electrical response and interfacial properties of oxide dielectrics on compound semiconductors.

ASSOCIATED CONTENT

Supporting Information.

The Supporting Information is available free of charge on the ACS Publication website.

Description of the used Mg precursor (Figure S1), description of the used Ca precursor (Figure S2), the scheme of the ALD system (Figure S3), Examples of X-Ray Reflectivity measurements of MgO and CaO film (Figure S4), XPS Mg 2p and O 1s fine scan of Al_2O_3(5 nm)/$Mg_{0.25}Ca_{0.75}O$(40nm)/GaN sample (Figure S5), XPS Mg 2p and O 1s fine scan of Al_2O_3(5 nm)/ $Mg_{0.51}Ca_{0.49}O$ (40nm)/GaN sample (Figure S6), XPS Mg 2p and O 1s fine scan of Al_2O_3(5 nm)/$Mg_{0.72}Ca_{0.28}O$(40nm)/GaN sample (Figure S7), Schematic drawing of band alignment of MgO/GaN under two extreme cases (Figure S8)

Corresponding Author

Prof. R. G. Gordon
E-mail: gordon@chemistry.harvard.edu

Present Addresses

Xiabing Lou
Cambridge Electronics Inc.
501 Massachusetts Avenue
Cambridge, MA 02139, USA

Sang Bok Kim
Center for Educational Research
Seoul National University
1 Gwanak-ro, Gwanak-gu, Seoul 08826, Korea

Author Contributions

The manuscript was written through contributions of all authors. All authors have given approval to the final version of the manuscript. X.G.‡ and X.B.L.‡ contributed equally.

Notes

The authors declare no competing interests.

ACKNOWLEDGMENT

This work was supported by the US National Science Foundation grant 1764338, the US Office of Naval Research contract N00014-10-1-0937, the US Department of Energy - Office of Science contract DE-AC36-08GO28308, and the Charles Stark Draper Laboratory, Inc. contract SC001-0000000950. This work was performed in part at the Harvard University Center for Nanoscale Systems (CNS), a member of the National Nanotechnology Coordinated Infrastructure Network (NNCI), which is supported by the National Science Foundation under NSF ECCS award no. 1541959.

References

(1) Long, R. D.; McIntyre, P. C. Surface Preparation and Deposited Gate Oxides for Gallium Nitride Based Metal Oxide Semiconductor Devices. *Materials* 2012, *5* (7), 1297-1335, DOI: 10.3390/ma5071297.
(2) Lee, K. A.; Min, B. K.; Byeon, Y. S.; Choi, J. H.; Jung, R. J.; Uhm, H. S.; Choi, E. H. Measurement of Energy Band Structure of MgO, MgSrO and MgCaO Thin Film by their

Secondary Electron Emission Coefficient due to Auger Neutralization. *Journal of Physics: Conference Series* 2013, *417*, 012009, DOI: 10.1088/1742-6596/417/1/012009.
(3) Lee, T.; Cheong, H.; Kwon, O.; Whang, K. Application of MgCaO Cathode Layer to Plasma Display Panel for High Luminous Efficacy. *IEEE Transactions on Electron Devices* 2013, *60* (1), 301-304, DOI: 10.1109/TED.2012.2224869.
(4) Zukawa, T.; Yoshino, K.; Oe, Y.; Kawarazaki, H.; Aoto, K.; Tanaka, Y.; Murai, R. In *13.5 L: Late‐News Paper: Development of MgCaO Protective Layer of Plasma Display Panels for Decreased Discharge Voltage*, SID Symposium Digest of Technical Papers, Wiley Online Library: 2012; pp 165-167.
(5) Stodilka, D.; Gerger, A. P.; Hlad, M.; Kumar, P.; Gila, B. P.; Singh, R.; Abernathy, C. R.; Pearton, S. J.; Ren, F. Alternative Magnesium Calcium Oxide Gate Dielectric for Silicon Carbide MOS Application. *MRS Proceedings* 2006, *911*, 0911-B14-03, DOI: 10.1557/PROC-0911-B14-03.
(6) Smith, D. L.; index, I. *Thin-Film Deposition: Principles and Practice*, McGraw-Hill Education: 1995.
(7) Kukli, K.; Ritala, M.; Sajavaara, T.; Hänninen, T.; Leskelä, M. Atomic layer deposition of calcium oxide and calcium hafnium oxide films using calcium cyclopentadienyl precursor. *Thin Solid Films* 2006, *500* (1-2), 322-329.
(8) Huang, R.; Kitai, A. H. Temperature‐dependence of the growth orientation of atomic layer growth MgO. *Applied physics letters* 1992, *61* (12), 1450-1452.
(9) Huang, R.; Kitai, A. The surface morphology of atomic layer deposited magnesia. *Journal of materials science letters* 1993, *12* (18), 1444-1446.
(10) Huang, R.; Kitai, A. H. Preparation and characterization of thin films of MgO, Al 2 O 3 and MgAl 2 O 4 by atomic layer deposition. *Journal of electronic materials* 1993, *22* (2), 215-220.
(11) Burton, B. B.; Fabreguette, F. H.; George, S. M. Atomic layer deposition of MnO using Bis(ethylcyclopentadienyl)manganese and H2O. *Thin Solid Films* 2009, *517* (19), 5658-5665, DOI: https://doi.org/10.1016/j.tsf.2009.02.050.
(12) Kim, E.; Han, Y.; Kim, W.; Choi, K. C.; Im, H.-G.; Bae, B.-S. Thin film encapsulation for organic light emitting diodes using a multi-barrier composed of MgO prepared by atomic layer deposition and hybrid materials. *Organic Electronics* 2013, *14* (7), 1737-1743, DOI: https://doi.org/10.1016/j.orgel.2013.04.011.
(13) Nilsen, O.; Fjellvåg, H.; Kjekshus, A. Growth of calcium carbonate by the atomic layer chemical vapour deposition technique. *Thin Solid Films* 2004, *450* (2), 240-247.
(14) Musgrave, C. B.; Gordon, R. G. Precursors for atomic layer deposition of high-k dielectrics. *Future Fab International* 2005, *18*, 126-128.
(15) Lou, X.; Zhou, H.; Kim, S. B.; Alghamdi, S.; Gong, X.; Feng, J.; Wang, X.; Ye, P. D.; Gordon, R. G. Epitaxial Growth of MgxCa1–xO on GaN by Atomic Layer Deposition. *Nano Letters* 2016, *16* (12), 7650-7654, DOI: 10.1021/acs.nanolett.6b03638.
(16) Kruger, M.; Williams, Q.; Jeanloz, R. Vibrational spectra of Mg (OH) 2 and Ca (OH) 2 under pressure. *The Journal of Chemical Physics* 1989, *91* (10), 5910-5915.
(17) Craft, H.; Collazo, R.; Losego, M.; Sitar, Z.; Maria, J.-P. Surface water reactivity of polycrystalline MgO and CaO films investigated using x-ray photoelectron spectroscopy. *Journal of Vacuum Science & Technology A: Vacuum, Surfaces, and Films* 2008, *26* (6), 1507-1510.

(18) Watts, J. F.; Wolstenholme, J. An introduction to surface analysis by XPS and AES. *An Introduction to Surface Analysis by XPS and AES, by John F. Watts, John Wolstenholme, pp. 224. ISBN 0-470-84713-1. Wiley-VCH, May 2003.* 2003, 224.
(19) Liu, P. *Reaction of water with UHV-cleaved MgO and CaO (100) surfaces: Microscopic, spectroscopic, and x-ray standing wave studies*, 1997.
(20) Kuang, W. J.; Tolner, H.; Li, Q. Cathode‐luminescence diagnostics of MgO, MgO: Si, MgO: Sc, and MgCaO. *Journal of the Society for Information Display* 2012, *20* (1), 63-69.
(21) Whited, R.; Flaten, C. J.; Walker, W. Exciton thermoreflectance of MgO and CaO. *Solid State Communications* 1973, *13* (11), 1903-1905.
(22) Doman, R.; Barr, J.; McNally, R.; Alper, A. Phase equilibria in the system CaO—MgO. *Journal of the American Ceramic Society* 1963, *46* (7), 313-316.
(23) Davies, P. K.; Navrotsky, A. Quantitative correlations of deviations from ideality in binary and pseudobinary solid solutions. *Journal of Solid State Chemistry* 1983, *46* (1), 1-22, DOI: https://doi.org/10.1016/0022-4596(83)90122-6.
(24) Li, H. D.; Zhang, X. N.; Zhang, Z.; Mei, Z. X.; Du, X. L.; Xue, Q. K. Epitaxial growth of CaO films on MgO(001) surface: Strain relaxation at the CaO⁄MgO heterointerface. *Journal of Applied Physics* 2007, *102* (4), 046103, DOI: 10.1063/1.2770826.
(25) Robertson, J.; Wallace, R. M. High-K materials and metal gates for CMOS applications. *Materials Science and Engineering: R: Reports* 2015, *88*, 1-41.
(26) Paisley, E. A.; Brumbach, M. T.; Shelton, C. T.; Allerman, A. A.; Atcitty, S.; Rost, C. M.; Ohlhausen, J. A.; Doyle, B. L.; Sitar, Z.; Maria, J.-P.; Ihlefeld, J. F. Nitride surface chemistry influence on band offsets at epitaxial oxide/GaN interfaces. *Applied Physics Letters* 2018, *112* (9), 092903, DOI: 10.1063/1.5013605.
(27) Supardan, S. N.; Das, P.; Major, J. D.; Hannah, A.; Zaidi, Z. H.; Mahapatra, R.; Lee, K. B.; Valizadeh, R.; Houston, P. A.; Hall, S.; Dhanak, V. R.; Mitrovic, I. Z. Band alignments of sputtered dielectrics on GaN. *Journal of Physics D: Applied Physics* 2019, *53* (7), 075303, DOI: 10.1088/1361-6463/ab5995.
(28) Robertson, J.; Falabretti, B. Band offsets of high K gate oxides on III-V semiconductors. *Journal of Applied Physics* 2006, *100* (1), 014111.
(29) Lou, X.; Gong, X.; Feng, J.; Gordon, R. Band-Offset Analysis of Atomic Layer Deposition La2O3 on GaAs(111), (110), and (100) Surfaces for Epitaxial Growth. *ACS Applied Materials & Interfaces* 2019, *11* (31), 28515-28519, DOI: 10.1021/acsami.9b08436.
(30) Robertson, J. Band offsets, Schottky barrier heights, and their effects on electronic devices. *Journal of Vacuum Science & Technology A* 2013, *31* (5), 050821, DOI: 10.1116/1.4818426.
(31) Robertson, J. Electronic Structure and Band Offsets of High-Dielectric-Constant Gate Oxides. *MRS Bulletin* 2002, *27* (3), 217-221, DOI: 10.1557/mrs2002.74.
(32) Bermudez, V. M. The fundamental surface science of wurtzite gallium nitride. *Surface Science Reports* 2017, *72* (4), 147-315, DOI: https://doi.org/10.1016/j.surfrep.2017.05.001.
(33) Janicki, Ł.; Gładysiewicz, M.; Misiewicz, J.; Klosek, K.; Sobanska, M.; Kempisty, P.; Zytkiewicz, Z. R.; Kudrawiec, R. Contactless electroreflectance studies of the Fermi level position at the air/GaN interface: Bistable nature of the Ga-polar surface. *Applied Surface Science* 2017, *396*, 1657-1666, DOI: https://doi.org/10.1016/j.apsusc.2016.12.013.
(34) Pang, H.; Ning, G.; Gong, W.; Ye, J.; Lin, Y. Direct synthesis of hexagonal Mg (OH) 2 nanoplates from natural brucite without dissolution procedure. *Chemical Communications* 2011, *47* (22), 6317-6319.

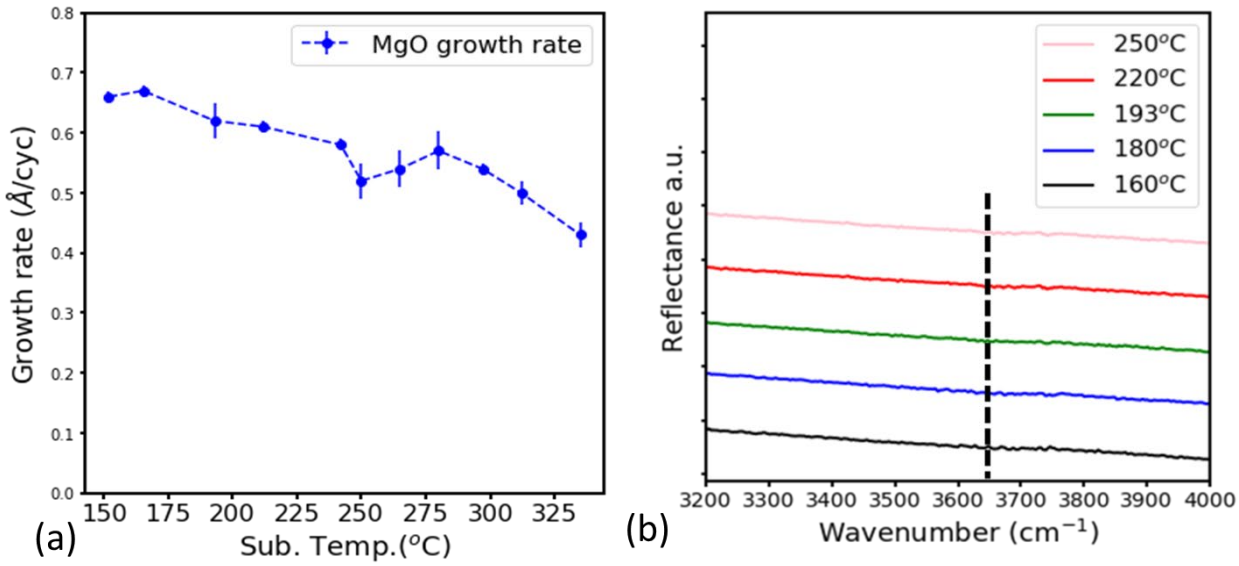

Figure 1.(a) MgO growth rate vs substrate temperature. (b) FTIR spectrum of MgO film deposited at different temperatures. The vertical dashed line labels the typical OH stretching peak position in $Mg(OH)_2$. [34]

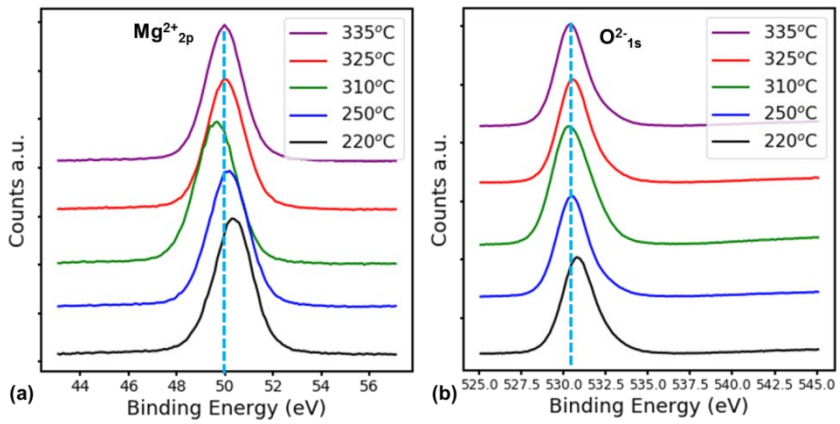

Figure 2.XPS spectra of MgO film. (a) Mg_{2p} scan. (b) O_{1s} scan

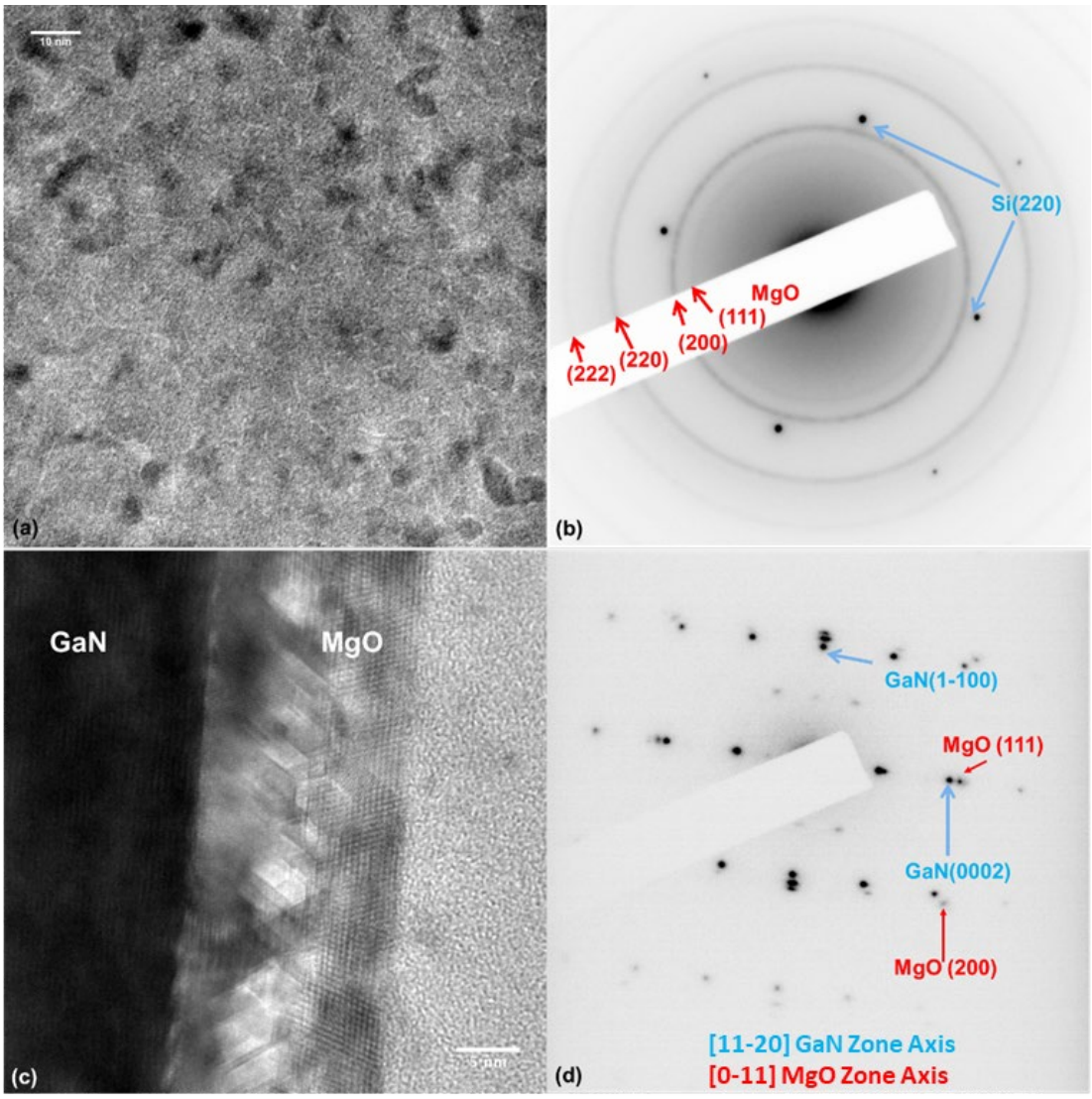

Figure 3. TEM of MgO. (a) HR-TEM image of 10 nm MgO film on SiN_x membrane covered by 5nm amorphous Al_2O_3. (b) Diffraction pattern with single crystalline Si(220) as reference. (c) HR-TEM cross section image of MgO/GaN(0001). (d) Diffraction pattern of (c).

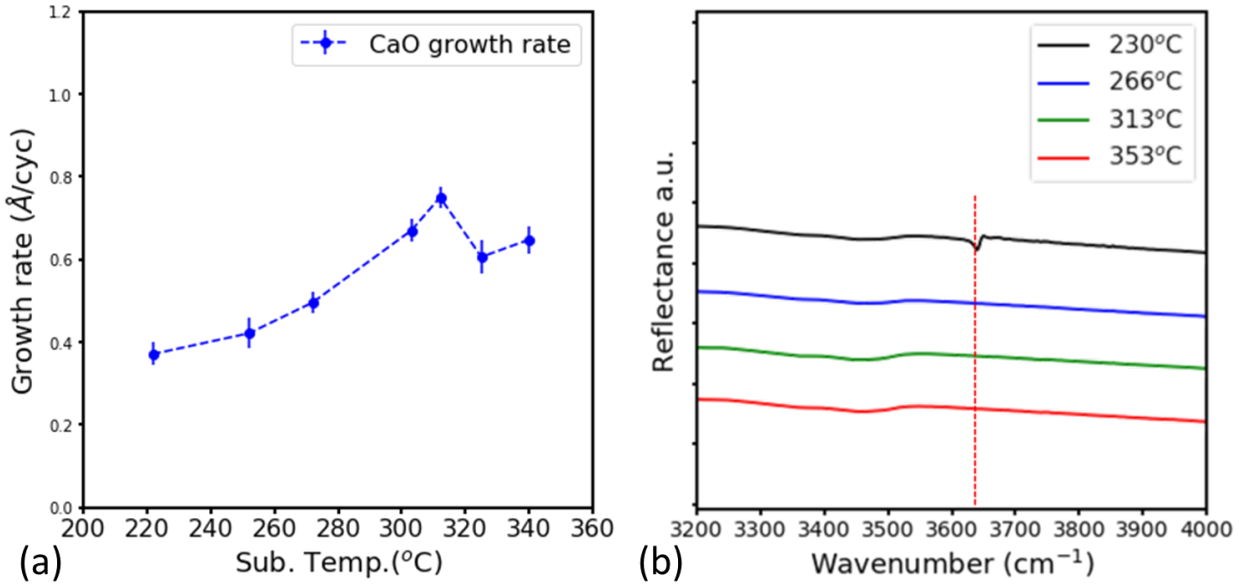

Figure 4. (a) CaO growth rate at different substrate temperatures. (b) IR spectrum of CaO film deposited at different substrate temperatures. The dashed red line indicates the expected OH group stretching adsorption**.**

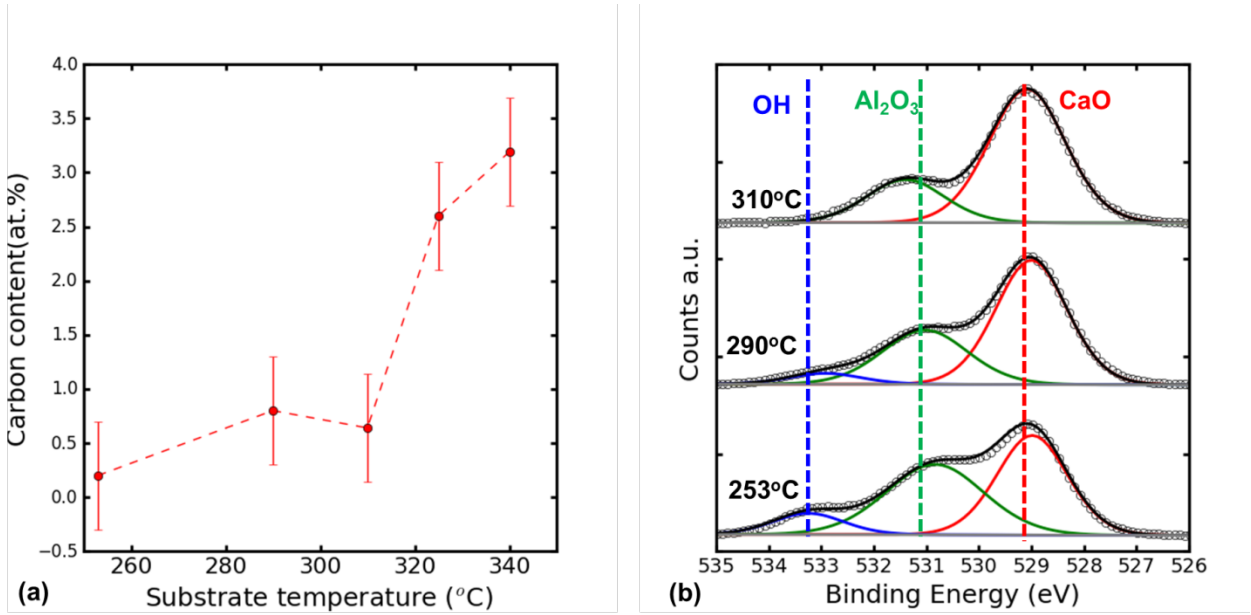

Figure 5. Temperature dependence of CaO film composition characterized by XPS. (a) Carbon content in CaO film at different deposition temperatures based on C1s peak area. (b) O1s scan of CaO films deposited at different temperatures.

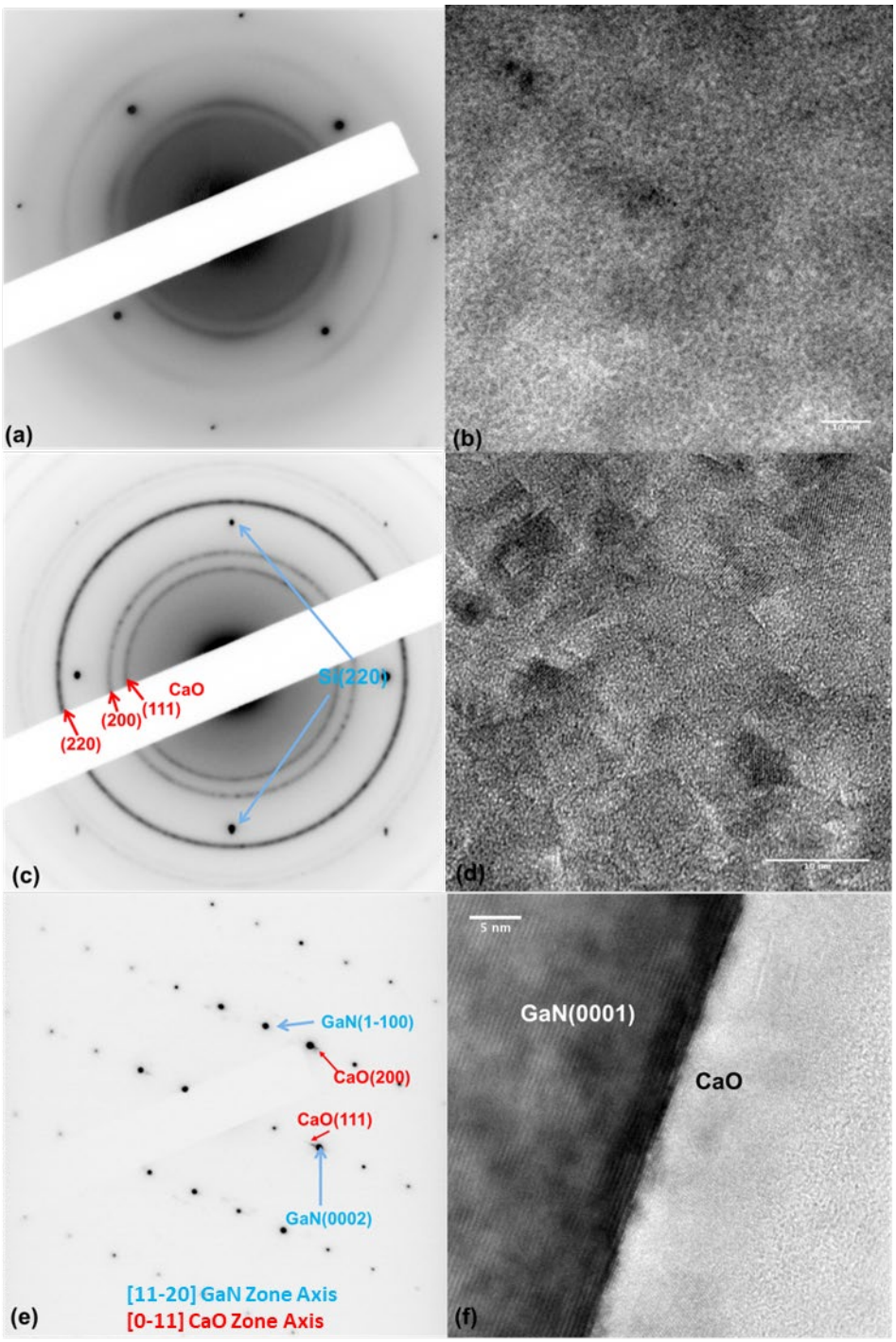

Figure 6. TEM images of ALD CaO film. (a) Diffraction pattern of CaO deposited at 273ºC. (b) HR-TEM image of CaO deposited at 273ºC. (c) Diffraction pattern of CaO deposited at 310ºC. (d) HR-TEM image of CaO deposited at 310ºC. (e) Diffraction pattern of CaO/GaN cross section. (f) HR-TEM of CaO/GaN cross section.

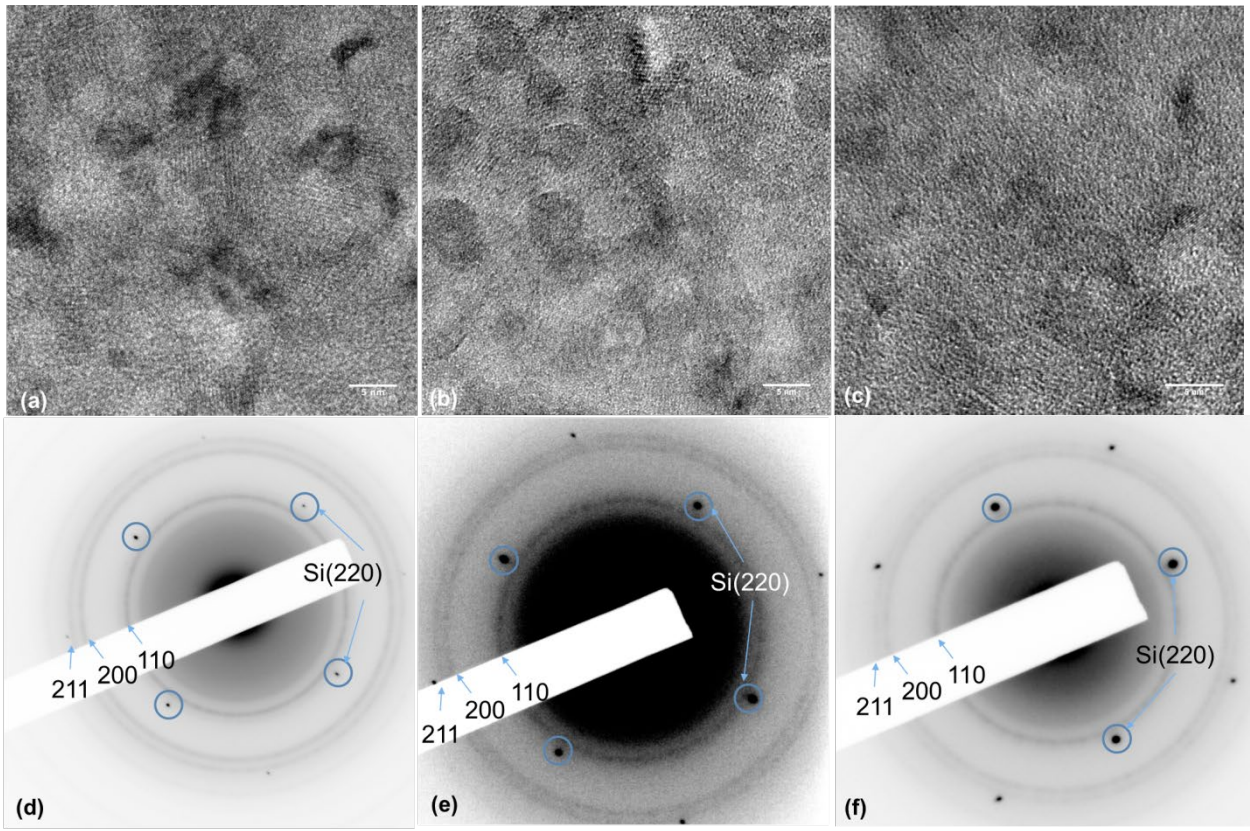

Figure 7. (a) Top view of $Mg_{0.25}Ca_{0.75}O/Si_3N_4$ membrane. (b) Top view of $Mg_{0.51}Ca_{0.49}O/Si_3N_4$ membrane. (c) $Mg_{0.72}Ca_{0.28}O/Si_3N_4$ membrane. (d) Diffraction pattern of $Mg_{0.25}Ca_{0.75}O$. (e) Diffraction pattern of $Mg_{0.51}Ca_{0.49}O$. (f) Diffraction pattern of $Mg_{0.72}Ca_{0.28}O$.

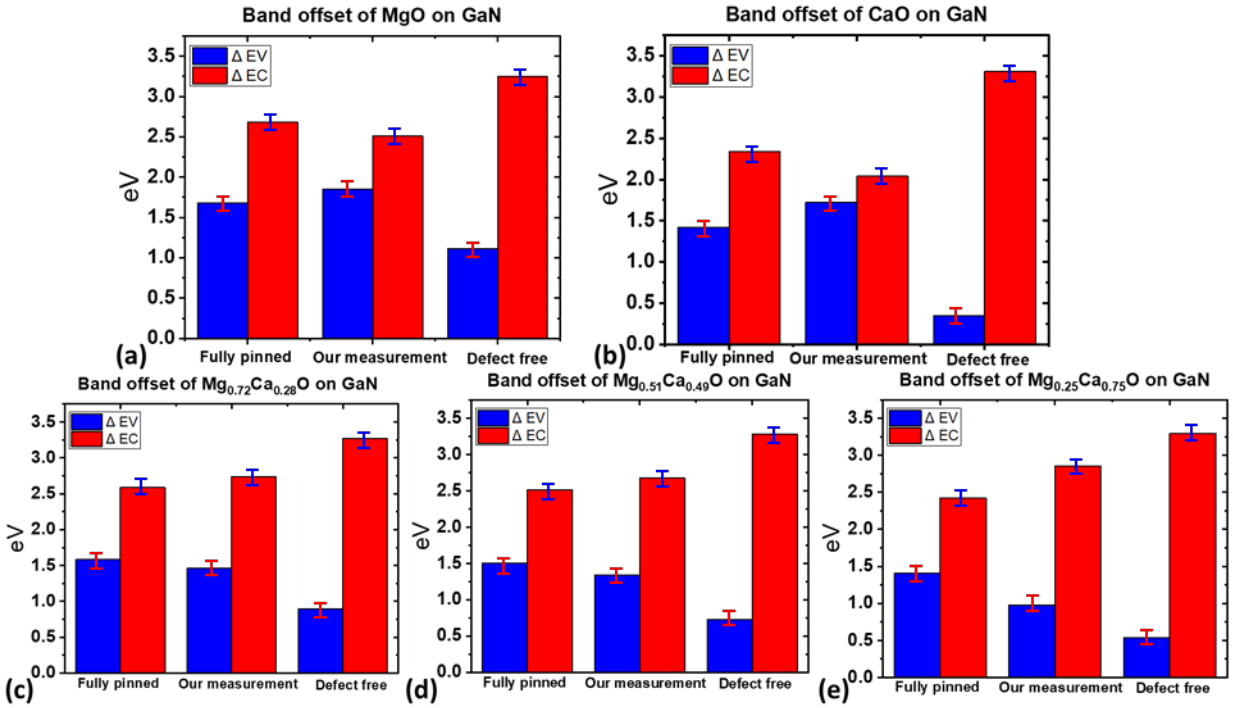

Figure 8. Band offset comparison between CNL model-predicted and XPS-measured $Mg_xCa_{1-x}O$ /GaN band offsets. Band offset of (a) MgO/GaN (b) CaO/GaN (c) $Mg_{0.72}Ca_{0.28}O$ /GaN (d) $Mg_{0.51}Ca_{0.49}O$ /GaN (e) $Mg_{0.25}Ca_{0.75}O$ /GaN

Table 1. Summary of ALD growth rates, compositions and lattice constants of different $Mg_xCa_{1-x}O$ films. The composition was measured by Rutherford back scattering (RBS). Lattice constants of $Mg_xCa_{1-x}O$ (222) were measured by HRXRD. MgO and CaO (222) lattice constants were from Crystallography Open Database.

Dosing ratio Mg:Ca	Average growth rate (Å/cycle)	Composition
CaO	**0.75 ± 0.015**	**CaO**
1:3	**0.5 ± 0.01**	**$Mg_{0.25}Ca_{0.75}O$**
1:2	**0.5 ± 0.01**	**$Mg_{0.51}Ca_{0.49}O$**
1:1	**0.6 ± 0.012**	**$Mg_{0.72}Ca_{0.28}O$**
MgO	**0.5 ± 0.01**	**MgO**

Table 2. Summary of XPS binding energy of $Mg_xCa_{1-x}O$ /GaN. All units are in eV. For CaO, E_{Ca2p} is used as $E_{oxide\ core}$. For all other compositions of $Mg_xCa_{1-x}O$ films, E_{mg2p} is used as $E_{oxide\ core}$.

	$E_{oxide\ core}$-E_{VBM} 40nm $Mg_xCa_{1-x}O$	E_{Ga3d}-E_{VBM} Bare GaN	E_{Ga3d} – $E_{oxide\ core}$ 2nm $Mg_xCa_{1-x}O$ /GaN	ΔE_V
MgO	**45.5 ± 0.05**	**17.88 ± 0.1**	**30.12 ± 0.04**	**1.85 ± 0.1**
$Mg_{0.72}Ca_{0.28}O$	**47.07 ± 0.05**	**17.88 ± 0.1**	**30.65 ± 0.04**	**1.46 ± 0.1**
$Mg_{0.51}Ca_{0.49}O$	**47.09 ± 0.05**	**17.88 ± 0.1**	**30.55 ± 0.04**	**1.34 ± 0.1**
$Mg_{0.25}Ca_{0.75}O$	**47.7 ± 0.05**	**17.88 ± 0.1**	**30.8 ± 0.04**	**0.98 ± 0.1**
CaO	**343.38 ± 0.08**	**17.88 ± 0.1**	**327.22 ± 0.06**	**1.72 ± 0.15**

Table 3. GaN and $Mg_xCa_{1-x}O$ properties. CNL value is defined as the energy difference between CNL and VBM.

	Ea(eV)	Eg(eV)	CNL(eV)
MgO	0.85	7.8	4.0
$Mg_{0.72}Ca_{0.28}O$	0.83	7.60	3.90
$Mg_{0.51}Ca_{0.49}O$	0.82	7.46	3.82
$Mg_{0.25}Ca_{0.75}O$	0.81	7.28	3.73
CaO	0.79	7.1	3.64
GaN	4.1	3.44	2.32